

Letters

Experimental Comparison of Traditional Phase-Shift, Dual-Phase-Shift, and Model-Based Control of Isolated Bidirectional DC–DC Converters

Hua Bai, Ziling Nie, and Chris Chunting Mi

Abstract—Three different control algorithms, traditional single-phase-shift control, dual-phase-shift control (DPSC), and model-based phase-shift control (MPSC), are implemented in a hardware setup and compared for a full-bridge-based isolated bidirectional dc–dc converter. The differences among their dynamic performance and steady-state operations are quantitatively analyzed. Experimental results showed good agreement with theoretical analysis. MPSC showed the best dynamic performance, while DPSC can eliminate reactive power under light-load conditions.

Index Terms—Bidirectional converter, dc–dc converter, full bridge, phase shift.

I. INTRODUCTION

IN half/full-bridge-based isolated bidirectional dc–dc converters, phase-shift control is the most widely used algorithm [1]–[3]. A proportional–integral (PI) controller is usually employed to realize the different modes of operation [4]. Bai *et al.* [5] focused on the application and optimization of phase-shift control in the microscopic perspective. Phase-shift plus pulsewidth modulation (PWM) algorithm was developed in [6] and [7] to accomplish more flexible control and validated for soft-switching, in aim of high-efficiency operations [8]–[10].

In an early paper, Bai and Mi proposed a dual-phase-shift control (DPSC) algorithm aiming at eliminating reactive power in a full-bridge isolated bidirectional dc–dc converter. Significant advantages were demonstrated compared to that using traditional single-phase-shift control (SPSC) [11]. In another paper, Bai *et al.* proposed a model-based phase-shift control (MPSC) [12] aiming at improving the dynamic performance of the converter. However, the studies were based on simulation and theoretical analysis. This letter is an extension of the previous work on DPSC, MPSC, and enhanced MPSC that also include dead-band compensation. In this letter, the two proposed algorithms, DPSC and enhanced MPSC, are validated

Manuscript received June 10, 2009; revised August 15, 2009. Current version published June 3, 2010. Recommended for publication by Associate Editor J. Biela.

H. Bai and C. C. Mi are with the Department of Electrical and Computer Engineering, University of Michigan, Dearborn, MI 48128 USA (e-mail: baihua@umd.umich.edu; chrismi@umich.edu).

Z. Nie is with the Department of Electrical and Computer Engineering, University of Michigan, Dearborn, MI 48128 USA, and also with the Huazhong University of Science and Technology, Wuhan 430074, China (e-mail: nieziling@163.com).

Color versions of one or more of the figures in this paper are available online at <http://ieeexplore.ieee.org>.

Digital Object Identifier 10.1109/TPEL.2009.2039648

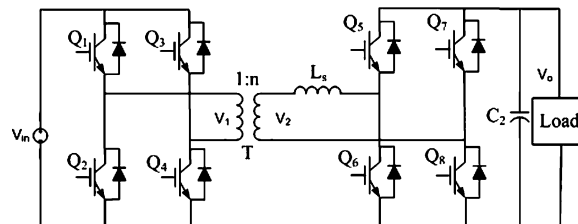


Fig. 1. Full-bridge isolated bidirectional dc–dc converter.

through experiments. In addition, the static and dynamic performances of the three control algorithms are compared through experiments.

II. COMPARISON OF THE OPERATION MODES

Fig. 1 shows the configuration of a full-bridge isolated bidirectional dc–dc converter [2], [3], where V_{in} and V_o are input and output voltage, respectively, n is the turns ratio of the transformer, Q_1 – Q_8 are the controllable switches, and L_s is the equivalent leakage inductance of the isolation transformer T .

The output power of the dc–dc converter, as shown in Fig. 1, can be expressed as the following for SPSC [4]:

$$P_1 = \frac{nV_1V_2}{2f_sL_s} D_1(1 - D_1) \quad (1)$$

where f_s is the switching frequency (in the following experiments $f_s = 10$ kHz), V_1 and V_2 are the voltages of the H-bridges on the primary and secondary sides, respectively, and D_1 is the phase-shift ratio.

The difference between SPSC and DPSC is that DPSC introduces another phase shift D_2 between Q_i and Q_{i+2} in Fig. 1 ($i = 1, 2, 5, 6$). Therefore, the width of the primary and secondary voltages will have variable pulsewidth, not fixed at one half period $T_s = 1/(2f_s)$. However, as depicted in [11], it is rather complicated to modulate two phase-shift controllers simultaneously. For simplicity, in the following analysis, DPSC fixes the phase shift between the voltage waveforms of the primary and secondary sides of the isolation transformer and only modulates the pulsewidth of the voltage by a PI controller. For example, when $D_1 = 0.5$, the operation modes of DPSC are shown in Fig. 2.

The power of the converter with DPSC is complicated [11]. For $D_1 = 0.5$ shown earlier, if $D_2 < 0.5$, then, the output power

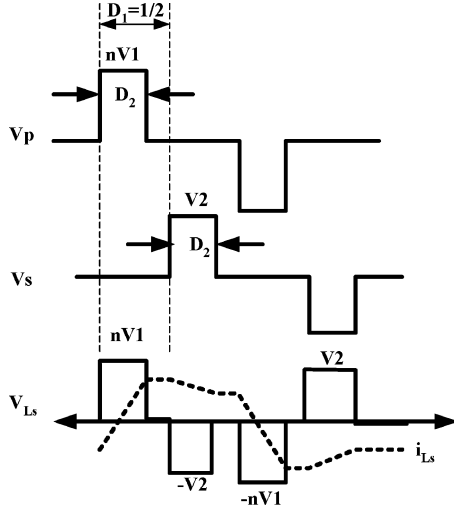


Fig. 2. Voltage waveforms of DPSC when $D_1 = 0.5$.

is as follows:

$$P_2 = \frac{nV_1 V_2}{4f_s L_s} D_2^2. \quad (2)$$

A third control algorithm to be compared in this letter is MPSC proposed in [12]. According to the previous study, a single PI control to modulate the phase shift has some limitations. The essence of this control is to predict the phase-shift angle based on load identification to supplement the PI modulator.

III. COMPARISON OF DYNAMIC RESPONSE

Bai *et al.* [12] demonstrated through simulation and theoretic analysis that MPSC has a better dynamic performance than SPSC. Experiments on the hardware platform presented in this letter validated this claim. The PI controller of these two control strategies has the same parameters. The input voltage is 30 V, output reference voltage is 70 V, $n = 2$, and leakage inductance is 54 μH . At some moment, the load of the system is switched from open circuit to a specific resistance. Fig. 3 shows the dynamic responses of the different control algorithms.

It can be seen from Fig. 3 that MPSC estimates the shift ratio D_1 needed to supply the power holding up the output voltage. When the load is changed, the predictor calculates the load power based on the feedback of output voltage and load current to estimate D_1 , according to (1). Therefore, the dynamic response of MPSC is better than that of the traditional SPSC.

It is worth to point out that the phase shift predicted by MPSC is not accurate enough when the switched load is light because the predicted D_1 is only an ideal phase shift, which does not include the influence of dead band. Bai *et al.* [5] pointed out that the dead band will erase part of the phase shift in the light-load operation. Therefore, besides predicted D_1 , an additional shift ΔD , compensating the dead-band time, is added to enhance the control.

This makes the output of the predictor to follow the actual required phase shift more precisely. The relationship between the erased angle (in seconds) and the real power is listed in

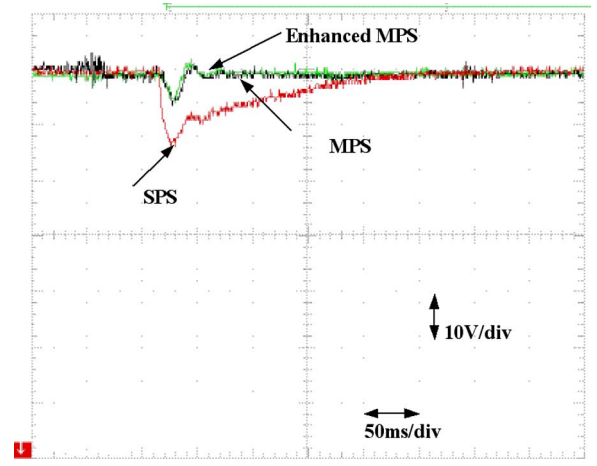


Fig. 3. Dynamic performance of SPSC and MPSC. Load changes from open circuit to 33 Ω (150 W).

the Table I. In practice, the erased angle is calculated, which is based on Table I. Based on Table I, the erased phase-shift angles by dead band based at different loads can be obtained. Therefore, the enhanced MPSC will use three parts to construct the phase shift, i.e., output of PI, phase-shift predictor, and dead-band compensator. The enhanced MPSC improves the dynamic performance in light-load operation. In heavy-load operations, the dead-band effect disappears. Therefore, the original MPSC and the enhanced MPSC are essentially the same. Experimental results showed that, under the same PI parameters, the enhanced MPSC always behaves the best.

Fig. 4 further compares the voltage drop during the transient process for different control algorithms. It can be seen that enhanced MPSC has the lowest voltage disturbance during the transient process.

IV. SMALL-SIGNAL MODEL AND STABILITY

In order to pursue the dynamic analysis, the linearized transfer function and small-signal models were set up in [12]. Although for the enhanced MPSC, the total phase-shift control is comprised of three independent controllers instead of a single PI controller, the output of two of the three controllers are maintained constant in the steady state, i.e., the output of phase-shift predictor and dead-band compensator. Therefore, the stability of the control strategy is determined by the PI controller.

Fig. 1 can be simplified, as shown in Fig. 5, where R_s is the source internal resistance. As pointed out in [12], the small-signal model of Fig. 5 is as follows:

$$\begin{bmatrix} \frac{d\langle v_1 \rangle}{dt} \\ \frac{d\langle v_2 \rangle}{dt} \end{bmatrix} = \begin{bmatrix} -\frac{1}{r_s C_1} & \frac{(D^2 - D)}{2L f_s C_1} \\ \frac{(-D^2 + D)}{2L f_s C_2} & -\frac{1}{RC_2} \end{bmatrix} \begin{bmatrix} \langle v_1 \rangle \\ \langle v_2 \rangle \end{bmatrix} + \begin{bmatrix} \frac{1}{r_s C_1} & \frac{2D - 1}{2L f_s C_1} \langle v_2 \rangle \\ 0 & \frac{-2D + 1}{2L f_s C_2} \langle v_1 \rangle \end{bmatrix} \begin{bmatrix} \langle v_s \rangle \\ \langle \Delta * D \rangle \end{bmatrix} \quad (3)$$

TABLE I
RELATIONSHIP BETWEEN POWER AND PHASE SHIFT ERASED BY DEAD BAND (Δt)

$i(0)$	Power P	Erased shift time Δt
$i(0) < -\frac{T_d}{L_s}(nV_1 + V_2)$	$P > \frac{nV_1V_2}{8f_sL_s} \left[1 - \left(\frac{1 - 4f_sT_d(1+m)}{m} \right)^2 \right]$	$\Delta t = 0$
$-\frac{T_d}{L_s}(nV_1 + V_2) \leq i(0) < 0$	$\frac{nV_1V_2}{8f_sL_s} \left[1 - \left(\frac{1}{m} \right)^2 \right] < P \leq \frac{nV_1V_2}{8f_sL_s} \left[1 - \left(\frac{1 - 4f_sT_d(1+m)}{m} \right)^2 \right]$	$\Delta t = T_d - \frac{1 - \sqrt{1 - \frac{8f_sL_sP}{nV_1V_2}}}{4(1+m)f_s}$
$i(0) \geq 0$	$P \leq \frac{nV_1V_2}{8f_sL_s} \left[1 - \left(\frac{1}{m} \right)^2 \right]$	$\Delta t = T_d$

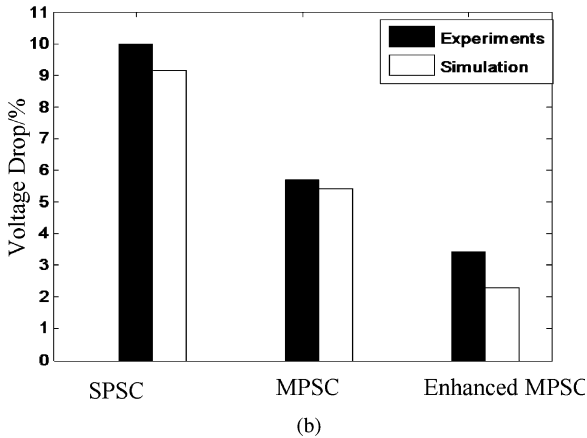
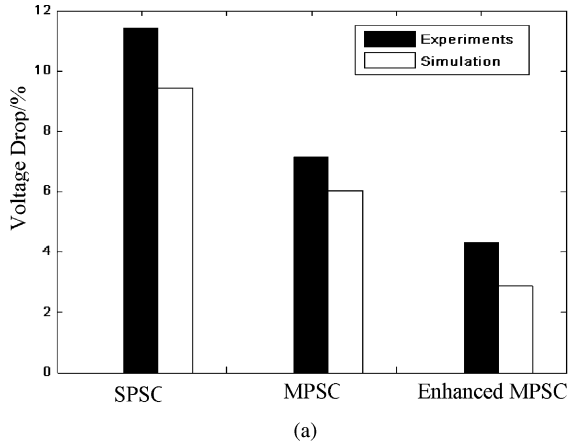


Fig. 4. Dynamic performance of SPSC, MPSC, and enhanced MPSC. (a) $K_p = 0.01$ and $K_i = 0.01$. (b) $K_p = 0.05$ and $K_i = 0.002$.

where $\langle v_1 \rangle$ and $\langle v_2 \rangle$ are the averaged voltage on the primary capacitor and secondary capacitor, respectively, D is the output of the PI controller, and Δ is the relative percentage of phase-shift variation. This output voltage ripple is directly affected by the variation of phase-shift duty ratio as follows:

$$\frac{\Delta v_2}{\langle v_2 \rangle} = \frac{-2D + 1}{4Lf_s^2C_2} \times \frac{\langle v_1 \rangle}{\langle v_2 \rangle} \Delta \times D. \quad (4)$$

However, if D is the composition of three controllers, i.e., the dead-band compensator, the phase-shift predictor, and the PI controller, then $D = D_{PS} + D_{DB} + D_{PI}$. Here D_{PS} is the output of phase-shift predictor, D_{DB} is the output of dead-band

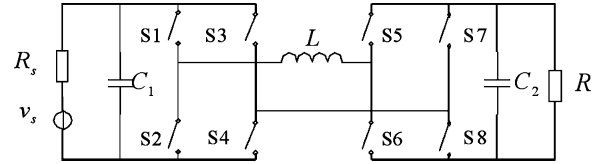


Fig. 5. Simplified circuit of a dual-active-bridge (DAB) dc-dc converter.

compensator, and D_{PI} is the output of the PI controller. In the steady state, D_{PS} and D_{DB} can be regarded as constant. Variation only occurs for the PI-controller output. Therefore, we rewrite (4) as follows:

$$\frac{\Delta v_2}{\langle v_2 \rangle} = \frac{-2D + 1}{4Lf_s^2C_2} \times \frac{\langle v_1 \rangle}{\langle v_2 \rangle} \Delta \times D_{PI}. \quad (5)$$

Assume that the relative variation of D_{PI} is the same. By comparing (5) to (4), D_{PI} is far less than D_{PS} and D_{DB} , as long as the power identification is accurate. Therefore, under the same relative vibration of D_{PI} , the variation of the output voltage is smaller than that generated by a traditional PI-based control. Therefore, the stability of MPSC and enhanced MPSC is better than the traditional SPSC.

V. DYNAMIC PERFORMANCE

Bai and Mi [11] compared the dynamic responses of these SPSC and DPSC algorithms and concluded that DPSC has shorter modulating process than SPSC. The conclusion is based on the assumption that there are two independent PI controllers to modulate the two phase shifts independently. In the experiments, it is difficult to synchronize these two PI controllers. In the following experiments, D_1 , phase shift between the primary and secondary side voltage waveforms of the transformer, is fixed to $1/3$, and D_2 , voltage pulsewidth, is changeable. Fig. 6(a) shows the experimental comparison of SPSC and DPSC, where line 1 is for SPSC, line 2 is DPSC with $D_2 = 1/2$, line 3 is DPSC with $D_2 = 1/3$, and line 4 is DPSC with $D_2 = 1/4$.

It can be seen from Fig. 6(a) that the dynamic response of SPSC is better than DPSC with fixed D_1 based on the same PI modulator. For line 2 and line 3, the modulating process of DPSC is always longer than SPSC. For line 4, the PI output D_2 even saturates. Simulation in Fig. 6(b) agrees with the aforementioned experiments.

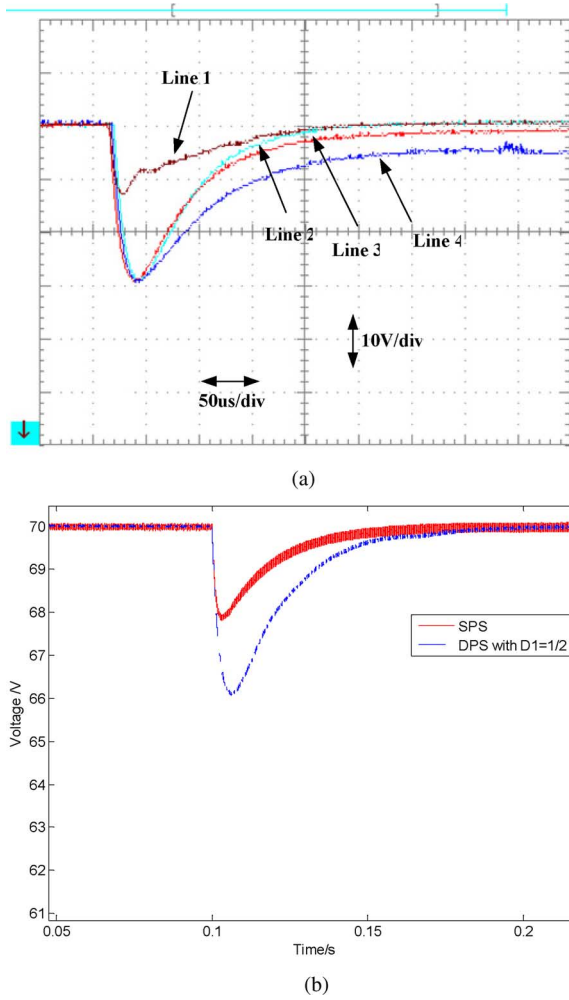


Fig. 6. Dynamic responses of DPSC and SPSC (from 60 to 164 W). (a) Measured dynamic responses of DPSC and SPSC. (b) Simulated dynamic responses of SPSC and DPSC.

Bai and Mi [11] used two PI controllers to accelerate the dynamic process of DPSC. This also contributes to the reason why DPSC in that paper has better dynamic response than SPSC. In the present hardware implementation, only one PI controller is used for simplicity. Up to now, coordinating two PI controllers is difficult to achieve. Further effort will be carried out in our future research.

VI. STEADY-STATE PERFORMANCE

In the steady-state operation, SPSC is the same with MPSC if their PI parameters are the same. Therefore, in this section, the focus is on the comparison of SPSC and DPSC by experiments.

Bai and Mi [11] pointed out that DPSC has higher efficiency than SPSC, especially at light-load conditions and when nV_1 is very different from V_2 . Under this circumstance, the reactive power of the system is considerably large. But under other circumstances when reactive power can be neglected, conclusions will change. In the following experiments, the turn's ratio of the isolation transformer is fixed at $n = 2$.

TABLE II
LOSS COMPARISON WHEN $nV_1 \ll V_2$

Control	V_1 (V)	I_1 (A)	V_2 (V)	Total Loss (W)
SPSC	50	15.1	188	755
DPSC, $D_2=1/2$	50	8.72	188	436
DPSC, $D_2=1/3$	50	6.86	190	343
DPSC, $D_2=1/4$	50	5.63	190	281.5

TABLE III
LOSS COMPARISON WHEN $nV_1 \approx V_2$

Control	V_1 (V)	I_1 (A)	V_2 (V)	Total Loss (W)
SPSC	100	0.24	199	24
DPSC, $D_2=3/4$	100	3.77	196	377
DPSC, $D_2=1/3$	100	2.65	196	265
DPSC, $D_2=1/4$	100	2.11	199	211

A. Loss and Efficiency Comparison

When nV_1 is far less than V_2 , (e.g., $V_1 = 50$ V, $V_2 = 190$ V), no-load operation, the measured loss of the system is shown in Table II. The experiment for $nV_1 \approx V_2$ is shown in Table III.

It can be seen from the aforementioned comparisons that losses under different operational modes are different. When $nV_1 \ll V_2$, the loss of DPSC is less than that of SPSC. When nV_1 is close to V_2 , results are reversed. Theoretically, D_1 is a small-valued number at light-load conditions. When $nV_1 < V_2$, the reactive power can be calculated based on the definition in [11]

$$Q = \frac{nV_1}{16f_s L_s^2} (V_2 - nV_1 - 2D_1 V_2)^2 \frac{1}{V_2 - nV_1}. \quad (6)$$

Assume $D_1 \rightarrow 0$ at light-load conditions, then

$$Q \rightarrow \frac{nV_1}{16f_s L_s^2} (V_2 - nV_1). \quad (7)$$

When $nV_1 > V_2$

$$Q = \frac{nV_1}{16f_s L_s^2} (V_2 - nV_1 - 2D_1 V_2)^2 \frac{1}{V_2 + nV_1}. \quad (8)$$

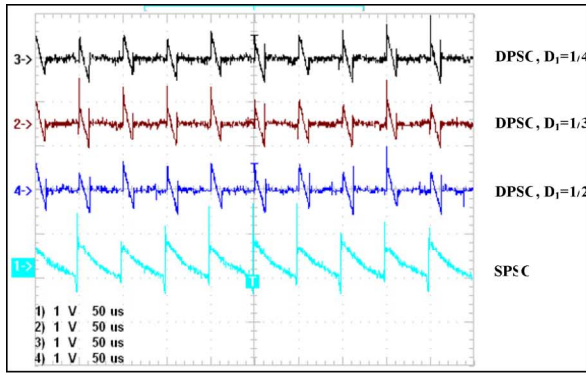
Assume $D_1 \rightarrow 0$, then

$$Q \rightarrow \frac{nV_1}{16f_s L_s^2} (V_2 - nV_1) \frac{V_2 - nV_1}{V_2 + nV_1}. \quad (9)$$

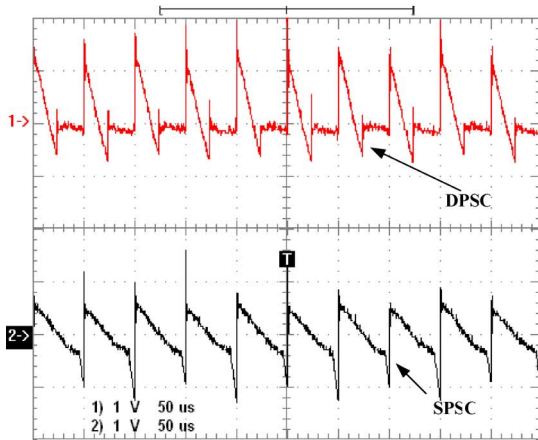
In Table III, V_2 is close to nV_1 , under light-load operation. Therefore, according to (7) and (9), the reactive power of the system is close to zero. Using DPSC to replace SPSC will not decrease reactive power, but will increase the current peak. At that time, DPSC will bring extra loss due to larger current, as pointed out in [11]. When V_2 increases, the reactive power of the system will also increase. Large reactive power brings large reactive current, which makes the reactive-power-associated loss dominant. Using DPSC at this condition will increase the system efficiency and decrease current peak by eliminating reactive power, as shown in Table II.

TABLE IV
EFFICIENCY COMPARISON WHEN $nV_1 > V_2$

Control	V_1 (V)	I_1 (A)	V_2 (V)	R (Ω)	η
SPSC	100	12.76	195	33	0.903
DPSC, $D_2=1/2$	100	18.79	190	33	0.582
DPSC, $D_2=1/3$	100	18.57	190	33	0.589
DPSC, $D_2=1/4$	100	14.86	189	33	0.728



(a)



(b)

Fig. 7. Voltage ripple of SPSC and DPSC. (a) Voltage ripple at no-load condition (experiments). (b) Voltage ripple at heavy-load condition (experiments).

In heavy-load operation, D_1 will increase. Therefore, the reactive power in (6) is further decreased. DPSC is not necessary in this case. The efficiency comparison is shown in Table IV for $V_1 = 100$ V, $V_2 = 180$ V, and load resistance $R = 33 \Omega$ (power 982 W).

Therefore, the best practice is to use SPSC when the system enters heavy-load operation and use DPSC at light-load operation. This experimental result is consistent with [11].

B. Comparison of Voltage Ripple

The output voltage ripple in the steady-state operation is due to the switching modes determined by the control algorithms and transient disturbance of the controller. Bai and Mi [11] pointed out that the output voltage ripple at steady state is a symbol of

reactive power exchange between the primary source and the output capacitance. For example, when $nV_1 < V_2$ at light-load condition, DPSC will decrease the reactive power; therefore, it is expected to have a smaller voltage ripple than that of SPSC. At heavy-load conditions, reactive power is reduced for all control algorithms; therefore, the voltage ripple of SPSC is comparable to that of DPSC.

Fig. 7 shows the output voltage ripple under different load conditions when $V_1 = 30$ V, $V_2 = 70$ V for DPSC and SPSC. Under light-load operation shown in Fig. 7(a), the voltage ripple of DPSC is smaller than that of SPSC. In one switching period, the voltage ripple of DPSC is discontinuous, lasting for a specific duty ratio. In other portion of the period, the output voltage remains constant. For SPSC, the output voltage is always fluctuating, which is caused by reactive power in the system. In Fig. 7(b) where the load is heavier, the output voltage ripple increases. At this circumstance, DPSC does not show advantages over SPSC. The experimental results agree with the theoretical analysis and simulations.

VII. CONCLUSION

In this letter, three control algorithms DPSC, MPSC, and enhanced MPSC have been validated through experiments and compared to SPSC. The dynamic responses and steady-state performance are evaluated and compared between experimental results and simulation results obtained in previous studies conducted by the authors.

Experiments showed good agreement with theoretical analysis and simulations. The dynamic response of MPSC and enhanced MPSC is best compared to SPSC and DPSC. In the steady state, DPSC can effectively eliminate reactive power and decrease steady-state voltage ripple. Due to the limitation of present experiments, some discrepancies between the experimental results and simulations exist. For example, due to the difficulty of coordinating two PI controllers, DPSC in this letter is quasi-closed-loop control and only one PI is used to adjust the pulsewidth of the primary and secondary voltages of the isolation transformer, while the phase shift is fixed. More advantages of DPSC are expected when dual PI modulators are applied.

REFERENCES

- [1] S. Han and D. Divan, "Bi-directional DC/DC converters for plug-in hybrid electric vehicle (PHEV) applications," in *Proc. IEEE APEC 2008*, Feb. 24–28, pp. 784–789.
- [2] S. Inoue and H. Akagi, "A bi-directional isolated DC/DC converter as a core circuit of the next-generation medium-voltage power conversion system," *IEEE Trans. Power Electron.*, vol. 22, no. 2, pp. 535–542, Mar. 2007.
- [3] Z. Haihua and A. M. Khambadkone, "Hybrid modulation for dual active bridge bi-directional converter with extended power range for ultracapacitor application," in *Proc. IAS 2008*, pp. 1–8.
- [4] C. Mi, H. Bai, C. Wang, and S. Gargies, "The operation, design, and control of dual h-bridge based isolated bidirectional DC-DC converter," *IET Power Electron.*, vol. 1, no. 3, pp. 176–187, 2008.
- [5] H. Bai, C. C. Mi, and S. Gargies, "The short-time-scale transient processes in high-voltage and high-power isolated bidirectional DC-DC converters," *IEEE Trans. Power Electron.*, vol. 23, no. 6, pp. 2648–2656, Nov. 2008.
- [6] D. Xu, C. Zhao, and H. Fan, "A PWM plus phase-shift control bidirectional DC-DC converter," *IEEE Trans. Power Electron.*, vol. 19, no. 3, pp. 666–675, May 2004.

- [7] L. Sun, D. Xu, M. Chen, and X. Zhu, "Dynamic model of PWM plus phase-shift (PPS) control bidirectional DC-DC converters," in *Proc. IAS 2005*, vol. 1, pp. 614–619.
- [8] H. Li, F. Z. Peng, and J. S. Lawler, "A natural ZVS medium-power bidirectional DC-DC converter with minimum number of device," *IEEE Trans. Power Electron.*, vol. 39, no. 2, pp. 525–535, Mar./Apr. 2003.
- [9] X. Wu, X. Xie, C. Zhao, Z. Qian, and R. Zhao, "Low voltage and current stress ZVZCS full bridge DC-DC converter using center tapped rectifier reset," *IEEE Trans. Ind. Electron.*, vol. 55, no. 3, pp. 1470–1477, Mar. 2008.
- [10] L. Zhu, "A novel soft-commutating isolated boost full-bridge ZVS-PWM DC-DC converter for bidirectional high power application," *IEEE Trans. Power Electron.*, vol. 21, no. 2, pp. 422–429, Mar. 2006.
- [11] H. Bai and C. Mi, "Eliminate reactive power and increase system efficiency of isolated bidirectional dual-active-bridge DC-DC converters using novel dual-phase-shift control," *IEEE Trans. Power Electron.*, vol. 23, no. 6, pp. 2905–2914, Nov. 2008.
- [12] H. Bai, C. Mi, C. Wang, and S. Gargies, "The dynamic model and hybrid phase-shift control of a dual-active-bridge converter," in *Proc. IECON 2008*, pp. 2840–2845.